

Impact of Increased Iron Content and Manganese Addition on Intermetallic Phases and Fatigue Resistance of AlSi7Mg0.6 Secondary Alloy

MIKOLAJČÍK Martin^{1, a *}, TILLOVÁ Eva^{1, b}, KUCHARIKOVÁ Lenka^{1, c} and
CHALUPOVÁ Mária^{1, d}

¹University of Žilina, Faculty of Mechanical Engineering, Department of Materials Engineering,
Univerzitná 8215/1, 010 26 Žilina, Slovak Republic

^amartin.mikolajcik@fstroj.uniza.sk, ^beva.tilova@fstroj.uniza.sk,
^clenka.kucharikova@fstroj.uniza.sk, ^dmaria.chalupova@fstroj.uniza.sk

Keywords: AlSi7Mg0.6, A357, Aluminium, Fatigue Properties, Effect of Fe and Mn

Abstract. One of the most often utilized metals in a variety of industries is aluminium alloy. Secondary aluminium alloys have drawn a lot of interest in recent years. Scrap aluminium may be recycled, which is good for the environment. In addition, compared to primary aluminium, it produces at a lower cost due to its lower energy requirement. Because it adversely affects their characteristics, secondary aluminium alloys' higher iron concentration presents the most frequent challenge. Manganese can be added to reduce its impact to some level. The objective of this research is to improve our knowledge of how iron and manganese affect the fatigue resistance of secondary aluminium alloys. Four alloys with various iron and manganese concentrations were tested to determine this impact.

Introduction

Secondary aluminium alloys are a class of materials that are derived from recycled aluminium and are widely used in various industries due to their high strength-to-weight ratio, excellent corrosion resistance, and cost-effectiveness. These alloys have been designed to meet the demanding requirements of various applications, including aerospace, transportation, construction, and packaging [1 - 3]. Although the addition of iron to aluminium alloys can provide benefits in terms of strength and fatigue resistance, it is most often considered to be an impurity. It is because iron also has a negative impact on the properties of the material. Iron can cause a reduction in ductility, which can make the material more brittle and prone to cracking. Additionally, the presence of iron leads to the formation of Al₅FeSi intermetallic compounds, which can act as stress concentrators and weaken the material. Iron can also increase the sensitivity of the material to corrosion, especially in aggressive environments. Therefore, it is important to carefully control the amount of iron added to aluminium alloys to ensure that its positive effects are maximized, and its negative effects are minimized [4 - 6]. Manganese can play a critical role in correcting the negative effects of iron in aluminium alloys. By forming stable intermetallic compounds with iron, manganese can prevent the formation of other, potentially harmful intermetallic compounds Al₅FeSi. Manganese can also help to increase the ductility of the material and improve its toughness, reducing the risk of cracking and failure. Finally, the combination of iron and manganese in aluminium alloys can provide a beneficial balance between strength, ductility, and corrosion resistance, making these alloys suitable for a wide range of applications [7 - 11]. The fatigue properties of aluminium alloys may also be impacted by the modification in the morphology of the intermetallic phases. Due to their sharp form, the plate-like Al₅FeSi particles are stress concentration points. These phases are also brittle, making them the ideal places for the development of fatigue cracks. Large Al₅FeSi particles also block the liquid flow channels as they solidify. Castings become more porous as a



result. Fatigue crack initiation is most frequently caused by casting defects beneath the casting surface. It can be expected that manganese should improve the experimental material's fatigue performance since its presence should reduce the number of shrinkage cavities [12 - 14]. According to research, more than 90% of engineering components that break are fractures caused by fatigue material. Fatigue fractures in transportation, such as those in rails, tire components, plane wings, and hulls of ships, are extremely dangerous since they are frequently associated with fatalities [15]. Therefore, the fatigue properties of materials need to be further investigated. This paper investigated how secondary AlSi7Mg0.6 cast aluminium alloy with a higher iron content responds to changes in iron and manganese levels in terms of its fatigue properties. The work is part of a project aimed at the study of secondary alloys with higher iron content.

Materials and Methods

We used secondary AlSi7Mg0.6 aluminium alloy, also known as A357 alloy, as an experimental material. The alloy had a higher iron content and was supplied in the form of rods (diameter of 20mm, length of 300mm) by UNEKO Zátor, a.s. These rods were manufactured by gravity casting into sand moulds at a temperature of 750°C and refined using ECOSAL Al 113S refining salt. We tested four alloys differing in the amount of iron and manganese in the chemical composition. We investigated the effect of manganese addition on the properties of materials at two different iron contents (0.75 wt.% and 1.25 wt.%). To increase iron and manganese content, we used pre-alloys AlFe75 and AlMn75. To purely study the impact of iron and manganese, we intentionally chose materials that were not heat treated. The supplier verified the complete chemical composition according to EN 10204 3.1, which is documented in Table 1.

Table 1. Chemical composition [wt.%]

Alloy	Al	Si	Mg	Fe	Mn	Ti	Cu
A	91.17	7.374	0.477	0.75	0.007	0.121	0.017
B	90.91	7.252	0.5	0.728	0.402	0.12	0.04
C	90.68	7.276	0.548	1.264	0.008	0.117	0.012
D	90.28	7.047	0.546	1.245	0.661	0.115	0.013

To prepare samples for metallographic and quantitative analysis, standard methods were applied. A Struers-CitoPress-1 was used to press the specimens into dentacryl after they had been cut from rods using an ATM Brillant 240 saw. Using a Struers TegraPol-15 automatic machine, the samples were ground and polished in five steps with varying sandpaper roughness, duration, and chemical environments. After that, 0.5% hydrofluoric acid was used to etch the samples. Metallographic and quantitative analyses were carried out using an optical microscope NEOPHOT-32 with NIS-Element 5.20 software. The aim of the quantitative analysis was to uncover how iron and manganese content affected the Fe-rich intermetallic phases' size and morphology. We also investigated the effect of chemical composition (addition of manganese) on the porosity of the castings.

Standard chip machining techniques were used to create the test rods for the fatigue tests. They measured 150mm in length, 12mm in width, and 8mm in diameter at their thinnest point. We used ROTOFLEX to analyze the alloys under test regarding their fatigue resistance. The test rods were bent while rotating, and the system kept track of how many cycles there were until failure. Each alloy was evaluated using a total of seven test rods at room temperature. The loads were 68, 78, and 88 MPa, and the test frequency was 32.1 Hz. The Department of Materials Engineering of UNIZA carried out all measurements.

Results

Fig.1. displays the outcomes of the metallographic analysis. We have determined the main structural elements: α -phase (substitutional solid solution of Si in Al) and eutectic (eutectic silicon crystals in the α -phase). We also observed ferrous intermetallic phases in the form of needles/plates (Al_5FeSi) and skeletons/Chinese scripts ($\text{Al}_{15}(\text{FeMnMg})_3\text{Si}_2$). The microstructure also contained Mg_2Si intermetallic phases, which do not have a significant effect in Al-Si alloys without heat treatment. Shrinkage cavities and pores were visible in the experimental material as casting defects.

Through quantitative analysis, the impact of iron and manganese on the porosity of castings was investigated. The analyses' findings are shown in Fig.2, Fig.3 and in Fig.4. The highest area proportion of casting defects was found in alloy D - 6.2%. In this material, the defects also have the largest dimensions ($21\,753.96\ \mu\text{m}^2$). The iron content does not affect the areal proportion or size of defects. The smallest casting defects are found in alloy B. Compared to alloys A and C, which are not alloyed with manganese, the pores in this alloy form a larger area fraction. It follows that manganese, especially at higher iron contents, has a negative effect on the area fraction of the formed casting defects. The effect of manganese on the size of the formed casting defects is also negative at higher iron contents.

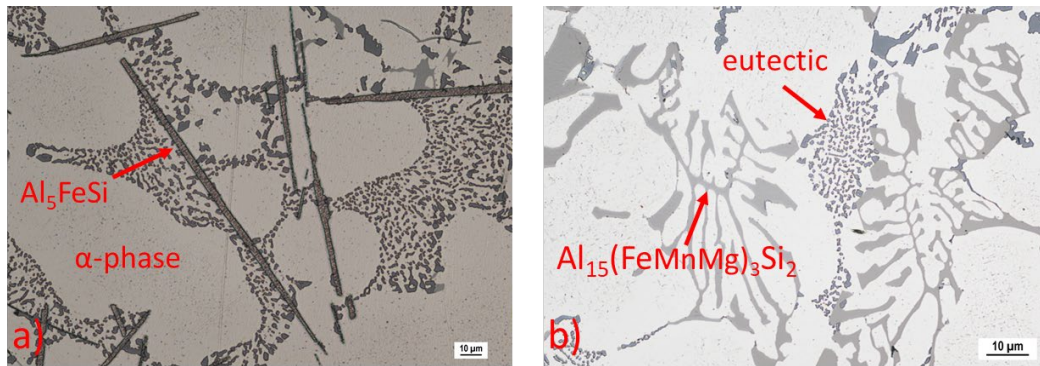


Fig.1. Identification of basic structural components in AlSi7Mg0.6 alloy.

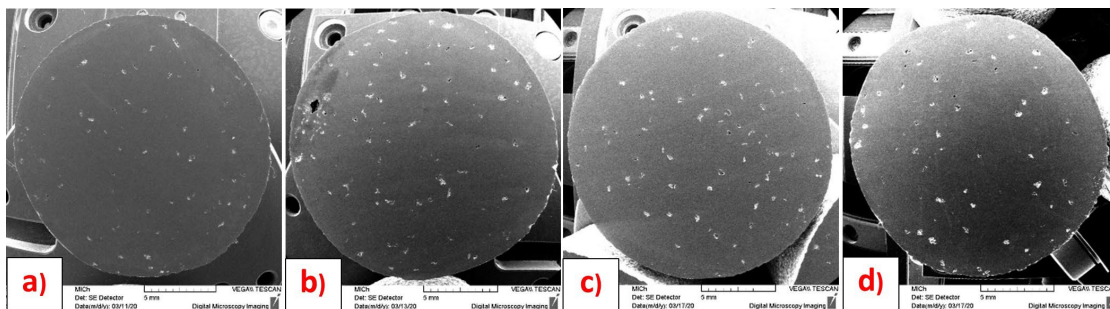


Fig.2. Effect of Mn on microporosity in AlSi7Mg0.6 alloy, SEM.

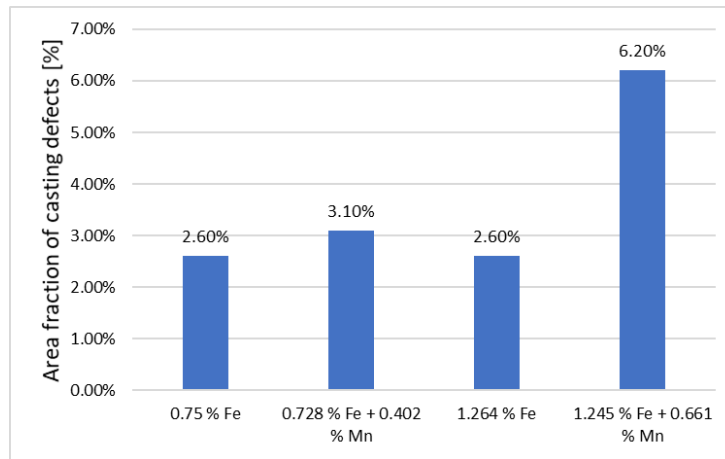


Fig.3. Effect of Fe and Mn on the area fraction of casting defects.

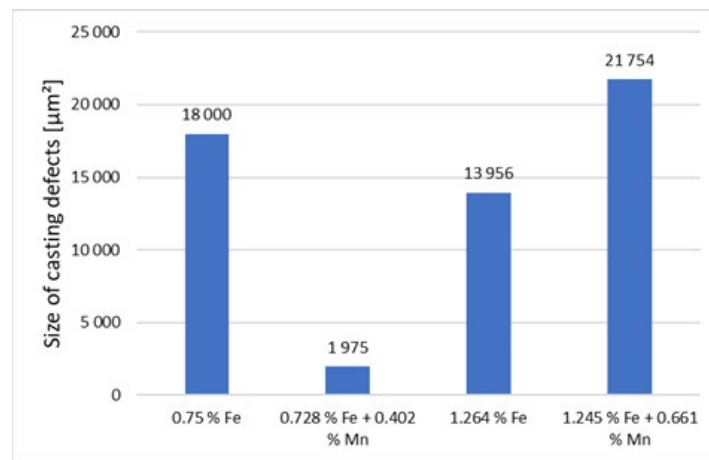


Fig.4. Effect of Fe and Mn on the size of casting defects.

The ferrous phases in AlSi7Mg0.6 alloys can take the form of thin plates (Al_5FeSi), which are visible as sharp needles on the cutting plane, skeletal structures ($Al_{15}(FeMnMg)_3Si_2$), or Chinese characters (also $Al_{15}(FeMnMg)_3Si_2$), depending on the chemical composition. The presence of manganese has a major impact on how the Fe-rich phases are shaped (Table. 2). Both the shape and the size of these phases undergo change. Al_5FeSi needle phases are formed in AlSi7Mg0.6 alloys, especially in the absence of Mn. In alloys B and D, which have been alloyed with manganese to correct the effect of iron, the ferrous phases in the form of plates are precipitated in much smaller amounts. At the same time, in the absence of manganese, the area fraction of needle phases in the structure increases with higher iron content. Therefore, the highest area fraction of Al_5FeSi phases in the structure is found in alloy C. The area fraction of Al_5FeSi needle phase grew from 2.2% to 3.5% with an increase in iron concentration from 0.75% to 1.25%. It significantly dropped from 2.2% to 0.7% and from 3.5% to 0.9% after manganese alloying.

In AlSi7Mg0.6 alloys, the presence or absence of manganese affects the size of the Al_5FeSi phases as well (Table 3). Shorter needles are created by adding manganese while keeping the iron amount the same. The length fell by about 55% (from 45.93 µm to 20.28 µm) at an iron concentration of 0.75%, and by about 20% (from 46.39 µm to 37.25 µm) with an iron content of about 1.25%. Longer Al_5FeSi needles occur because manganese alloyed alloys have a larger iron concentration. The influence of iron concentration on needle length is minimal in the case of alloys without manganese.

Table 2. Effect of Fe and Mn on the area fraction of Al₅FeSi phase

Alloy	A	B	C	D
Area fraction of Al ₅ FeSi phase	2.2 %	0.7 %	3.5 %	0.9 %

Table 3. Effect of Fe and Mn on length of Al₅FeSi phases

Alloy	A	B	C	D
Length of Al ₅ FeSi phases [μm]	45.83	20.28	46.39	37.25

When manganese is present, skeletal iron phases and Chinese script-shaped phases (Al₁₅(FeMnMg)₃Si₂) are found in the microstructure. Phases with the stated morphology were not found in the microstructure of alloys A and C because manganese is only in minimal amounts in these materials. In alloys with a higher manganese concentration (melts B and D), the area percentage of skeleton phases has a similar value (Fig.5). Alloy D, which contains more iron, had a slightly larger proportion of these phases.

The fatigue properties of the experimental alloys were studied using cyclic bending loads under rotation. Figures 6 - 8 show a comparison of the Wöhler curves for the experimental alloys (stress amplitude (σ) vs the number of cycles to fracture (N)). All the curves are decreasing in character. The number of cycles to fracture rises as the load amplitude lowers from 88 MPa to 68 MPa, showing an exponential decrease with an asymptotic approach to zero.

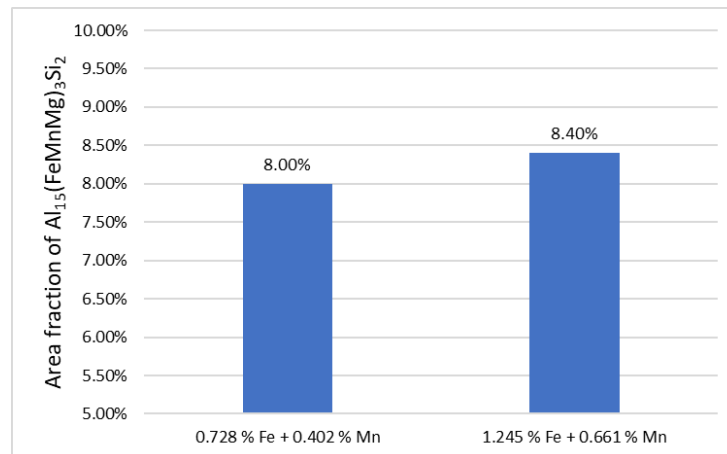


Fig.5. Effect of Fe and Mn on area fraction of Al₁₅(FeMnMg)₃Si₂ phases.

We discovered that the effect of iron changes with the load (Fig.6). Iron has a negative effect at higher loads. The test bars resisted cyclic loads of fewer than 10⁵ cycles, independent of their iron content. This is because the fatigue crack's initiation and spread are accelerated by the fracture of brittle Al₅FeSi particles. In contrast, at lower loads, the higher iron concentration has a beneficial effect on fatigue resistance. This is likely caused by the Al₅FeSi plate-like phases in the matrix of alloy C, which have a different orientation, are much longer than in alloy A, and slow down fatigue fracture propagation. It would be necessary to do more experiments with more test rods to determine the impact of iron more precisely.

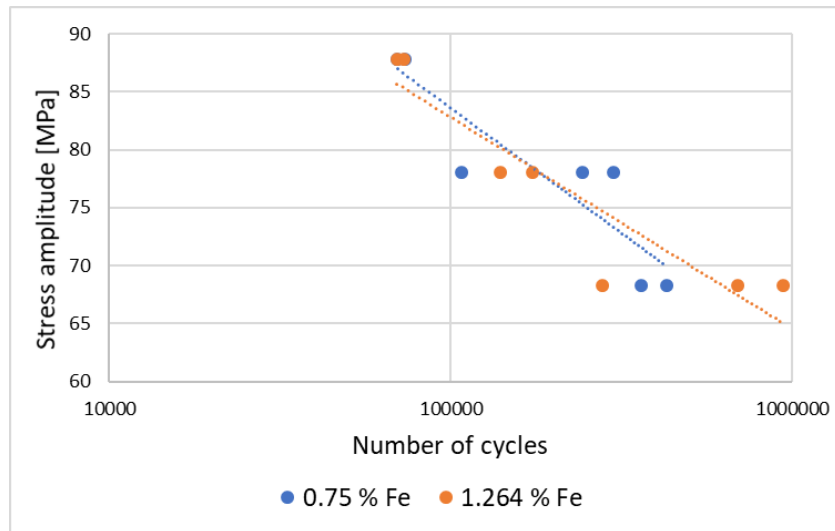


Fig.6. Effect of Fe on the fatigue resistance of AlSi7Mg0.6 alloy.

Manganese has a beneficial impact on the fatigue resistance of the AlSi7Mg0.6 alloy, as seen in Fig.7. and Fig.8. The fatigue curves shifted to the right as a result. This demonstrates that alloys with Mn can resist more cycles with the same amplitude of loading. Manganese was found to have a stronger impact on alloys with less iron. The beneficial effect of manganese was especially evident at greater loads at high iron contents. Samples withstand a higher number of cycles (Fig.7). In alloys with higher iron content (Fig.8), the effect of manganese was negative at a load of 68 MPa, which is probably related to an increase in porosity (Fig.3). The samples withstand a significantly lower number of cycles.

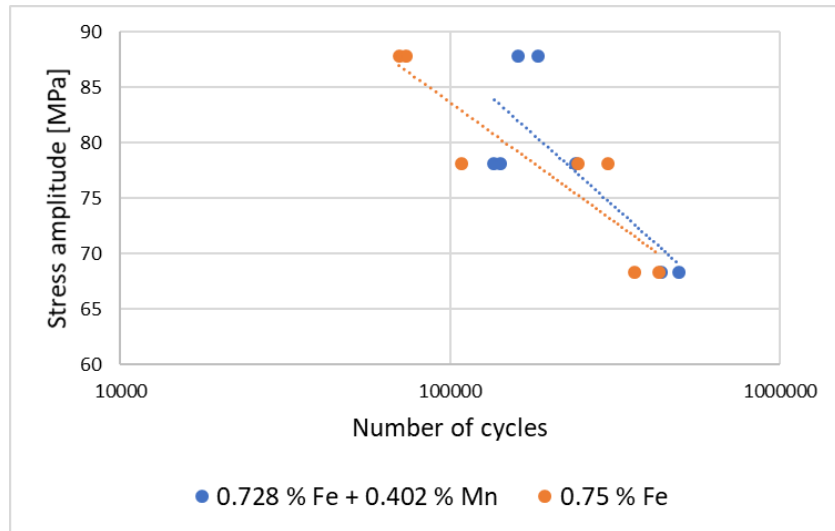


Fig.7. Effect of Mn on fatigue resistance of AlSi7Mg0.6 alloy.

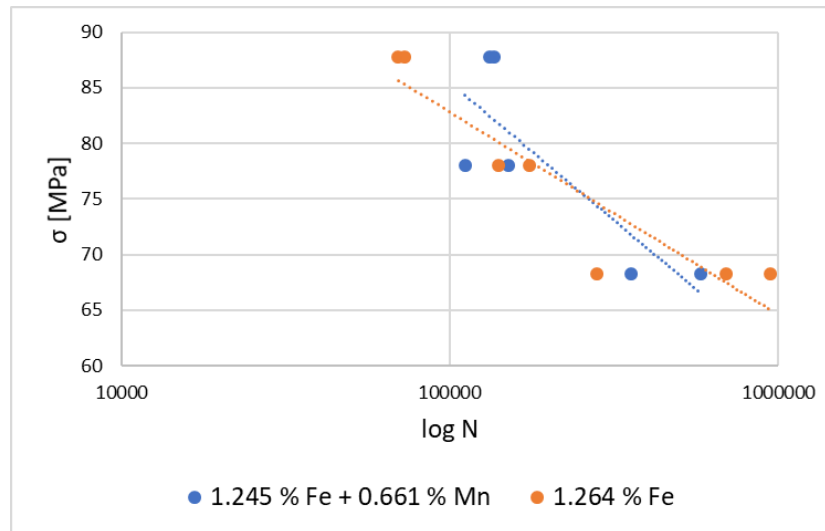


Fig.8. Effect of Mn on the fatigue resistance of AlSi7Mg0.6 alloy.

Summary

The following conclusions can be drawn from the experimental results:

- Pore and shrinkage cavities are more likely to occur when manganese levels are higher. With higher iron content and manganese doping, the casting defects were of the largest size.
- The plate/needle-like phases of Al_5FeSi are more widespread in alloys without significant manganese content. With an increase in Fe content, these phases become more common.
- Manganese reduces the number and dimensions (especially the length) of Al_5FeSi needles and contributes to the formation of skeleton-shaped $Al_{15}(FeMnMg)_3Si_2$ phases or Chinese scripts. The amount of $Al_{15}(FeMnMg)_3Si_2$ phase slightly increases as the percentage of Fe rises.
- Higher manganese content has a positive effect on the fatigue properties of the experimental material, which was manifested by a shift of the fatigue curves to the right. It means that Mn doped alloys resist a higher number of cycles at the same loading amplitude. Manganese was found to have a stronger impact on alloys with less iron. In higher iron content alloys, the effect of manganese was negative at lower loads. The effect of iron on fatigue resistance depends on the magnitude of the load. It would be necessary to complete the measurements with more test bars in order to assess the impact of Fe and Mn on the fatigue parameters of the AlSi7Mg0.6 alloy more precisely.

Acknowledgements

The research was supported by Grand Agency of Ministry of Education of Slovak Republic and Slovak Academy of Sciences, project KEGA 004ŽU-4/2023, project to support young researchers at UNIZA, ID project 12715 (Kuchariková) and project 313011ASY4 “Strategic implementation of additive technologies to strengthen the intervention capacities of emergencies caused by the COVID-19 pandemic”.

References

- [1] Y-Ch. Tzeng et al. Effect of Trace Be and Sc Additions on the Mechanical Properties of A357 Alloys, *Metals* 8 (2018) art.194. <https://doi.org/10.3390/met8030194>
- [2] H. Nunes et al. Adding Value to Secondary Aluminium Casting Alloys: A Review on Trends and Achievements, *Materials* 16 (2023) art.895. <https://doi.org/10.3390/ma16030895>

- [3] I. Švecová et al. Improving the quality of Al-Si castings by using ceramic filters, *Prod. Eng. Arch.* 26 (2020) 19-24. <https://doi.org/10.30657/pea.2020.26.05>
- [4] J. Kasińska et al. The Influence of Remelting on the Properties of AlSi9Cu3 Alloy with Higher Iron Content, *Materials* 13 (2020) art.575. <https://doi.org/10.3390/ma13030575>
- [5] B. Chen et al. The Effect of Cu Addition on the Precipitation Sequence in the Al-Si-Mg-Cr Alloy, *Materials* 15 (2022) art.8221. <https://doi.org/10.3390/ma15228221>
- [6] L. Pastierovičová et al. Quality of automotive sand casting with different wall thickness from progressive secondary alloy, *Prod. Eng. Arch.* 28 (2022) 172-177. <https://doi.org/10.30657/pea.2022.28.20>
- [7] A. Bakedano et al. Comparative Study of the Metallurgical Quality of Primary and Secondary AlSi10MnMg Aluminium Alloys, *Metals* 11 (2021) art.1147. <https://doi.org/10.3390/met11071147>
- [8] M. Gnatko et al. Purification of Aluminium Cast Alloy Melts through Precipitation of Fe-Containing Intermetallic Compounds, *Metals* 8 (2018) art.796. <https://doi.org/10.3390/met8100796>
- [9] L. Ceschini et al. Influence of Sludge Particles on the Fatigue Behaviour of Al-Si-Cu Secondary Aluminium Casting Alloys, *Metals* 8 (2018) art.268. <https://doi.org/10.3390/met8040268>
- [10] L. Stanček et al. Structure and properties of silumin castings solidified under pressure after heat treatment, *Met. Sci. Heat Treat.* 56 (2014) 197-202. <https://doi.org/10.1007/s11041-014-9730-0>
- [11] B. Vanko, L. Stanček. Utilization of heat treatment aimed to spheroidization of eutectic silicon for silumin castings produced by squeeze casting, *Arch. Foundry Eng.* 12 (2012) 111-114. <https://doi.org/10.2478/v10266-012-0021-1>
- [12] M. Brochu et al. High cycle fatigue strength of permanent mold and rheocast aluminium 357 alloy. In: *Int. J. Fatigue* 32 (2010) 1233-1242. <https://doi.org/10.1016/j.ijfatigue.2010.01.001>
- [13] D. Závodská et al. The Effect of Iron Content on Microstructure and Porosity of Secondary AlSi7Mg0.3 Cast Alloy, *Period. Polytech. Transp. Eng.* 47 (2018) 283-289. <https://doi.org/10.3311/PPtr.12101>
- [14] M. Oberreiter et al. A Probabilistic Fatigue Strength Assessment in AlSi-Cast Material by a Layer-Based Approach, *Metal* 12 (2022) art.784. <https://doi.org/10.3390/met12050784>
- [15] L. Kuchariková et al. High-cycles Fatigue of Different Casted Secondary Aluminium Alloy, *Manuf. Technol.* 17 (2017) 756-761. <https://doi.org/10.21062/ujep/x.2017/a/1213-2489/MT/17/5/756>